No.102 **May 2022**

ISSN 0917-2211

Variable Star Bulletin

Analysis of TESS observations of V844 Her during the 2020 superoutburst

Taichi Kato[1]

tkato@kusastro.kyoto-u.ac.jp

[1] Department of Astronomy, Kyoto University, Sakyo-ku, Kyoto 606-8502, Japan

Received 2022 May 10

Abstract

I analyzed Transiting Exoplanet Survey Satellite (TESS) observations of the 2020 superoutburst of the SU UMa-type dwarf nova V844 Her. This object showed "textbook" superhump stages A, B and C confirmed by modern satellite observations. The resultant figure can be used for an illustration of the concept of superhump stages under the Creative Commons (CC-BY-NC) licence. During the growing phase of superhumps, the period was initially close to, but slightly longer than the orbital period. Observers should pay attention to the presence of such a phenomenon not to confuse the phenomenon with early superhumps seen in WZ Sge stars. After the superoutburst, superhumps were detected for additional 18 d with the same period and no orbital signal was detected. Small wiggles with a period of ∼0.5 d were recorded in the post-superoutburst phase and they may be the same phenomenon recorded in the Kepler data of the SU UMa star V585 Lyr.

Superhump stages A, B and C in SU UMa-type (including WZ Sge-type) dwarf novae were established in Kato et al. (2009) [for general information of cataclysmic variables and dwarf novae, see e.g. Warner (1995)]. In Kato et al. (2009), a figure representing stage A–C was shown based on the 2000 ground-based observation of SW UMa (in their figure 3), and this figure or its revision (figure 1 in Kato and Osaki 2013b) has been used in various papers to explain the concept of superhump stages. The data for SW UMa, however, were rather old and there were gaps in the observations. Although a figure based on continuous satellite observations had been desired, only long cadence (LC) Kepler data of V585 Lyr could be used nine years ago (Kato and Osaki 2013a). The Kepler LC data were insufficient to draw an $O-C$ diagram directly and Kato and Osaki (2013a) had to reconstruct the original light curve by introducing a Bayesian method.

The aim of this paper is to provide a corresponding figure based on modern data which is equivalent to figure 3 in Kato et al. (2009). I used Transiting Exoplanet Survey Satellite (TESS) observations (Ricker et al. 2015)[1] of the 2020 superoutburst of V844 Her, which is an SU UMa-type dwarf nova very similar to SW UMa (Antipin 1996; Kato and Uemura 2000; Oizumi et al. 2007) and has a similar short orbital period of 0.054643 d (Thorstensen et al. 2002). In addition to the greatly improved coverage and statistics, the figures in this paper are provided under the Creative Commons licence (CC-BY-NC) and can be used without consideration of the copyright of the publisher. First of all, I show figure 1. This figure clearly demonstrate the "textbook" example of superhump stages in a short-period SU UMa-type dwarf nova. I describe how I obtained this figure.

The TESS data of V844 Her during the 2020 superoutburst and early post-superoutburst phase are shown in figure 3. The superhump maxima were obtained by the template fitting method introduced in Kato et al. (2009) and the quality of the $O-C$ values is the same as in the series of "Pdot papers" (Kato et al. 2009, 2010, 2012, 2013, 2014b,a, 2015, 2016, 2017, 2020) for a collection of SU UMa/WZ Sge stars and which were

[1] <https://tess.mit.edu/observations/>. The full light-curve is available at the Mikulski Archive for Space Telescope (MAST, <http://archive.stsci.edu/>).

Table 1: Superhump period in V844 Her

Stage	E	BJD−2400000	Period (d)	$P_{\rm dot} \times 10^5$
A	0–38	58956.11–58958.25	0.056425(43)	44(13)
B	38–188	58958.25–58966.64	0.055928(9)	9.7(2)
C	188–297	58966.64–58972.71	0.055638(12)	−9.0(12)
Post-superoutburst	–	58972–58975	0.05554(4)	–
Post-superoutburst	–	58975–58978	0.05554(4)	–
Post-superoutburst	–	58978–58981	0.05554(4)	–
Post-superoutburst	–	58984–58987	0.05553(6)	–
Post-superoutburst	–	58987–58990	0.05558(8)	–

homogeneously determined using the same method. This method has an advantage of much higher signal-to-noise and thereby higher precision in determining maxima than picking up the peaks (Kato et al. 2009). The representative superhump periods in different superhump stages are given in table 1. For stages A, B and C, the mean period (P) and the period derivative ($P_{\rm dot} = \dot{P}/P$) are given. For the post-superoutburst stage, individual maxima could not be obtained by the template fitting method and the periods were determined using the Phase Dispersion Minimization (PDM, Stellingwerf 1978) method after removing long-term trends by locally-weighted polynomial regression (LOWESS: Cleveland 1979). The errors of periods by the PDM method were estimated by the methods of Fernie (1989) and Kato et al. (2010). I used 3-d windows considering the beat period between $P_{\rm orb}$ and the superhump period ($P_{\rm SH}$). Using $P_{\rm orb}$ and the period of stage A superhumps, the fractional superhump excess in frequency $\epsilon^* = 1 - P_{\rm orb}/P_{\rm SH}$ for stage A is 0.0316(7). This value corresponds to a mass ratio of q=0.086(2) using the stage A superhump method (Kato and Osaki 2013b; Kato 2022). The location on the $P_{\rm orb}$–q plane is shown in figure 2, on which V844 Her was plotted on figure 11 in Kato (2022).

The variation of the superhump profile is shown in figures 4, 5 and 6. The most important finding in this paper is in the development of superhumps in stage A (figure 4). Although stage A with growing amplitudes is clearly present in figure 1, the $O-C$ variation is not on a straight line. The reason has been clarified in figure 4: before stage A superhump started to develop fully, there was a phase when the period was close to (but slightly longer than) the orbital period. The average epoch of humps in this phase, however, was on the smooth extension of stage A superhumps (see figure 1). It was not clear whether this feature is special to V844 Her or it is a general phenomenon. Observers should pay attention to the presence of this phenomenon not to confuse this variation with early superhumps seen in WZ Sge stars (Kato 2015). This is particularly true when the period is identified only by frequency(period) analysis and no $O-C$ analysis is performed.

During the post-superoutburst phase (figure 6), superhumps rapidly decayed. The superhump signal, however, was detected with the same period by the PDM method for 18 d in the post-superoutburst phase (table 1; the gap between BJD 2458981 and 2458984 was due to the gap in TESS observation). No orbital signal was detected during the post-superoutburst phase as in the case of V585 Lyr. The small wiggles with a period of ∼0.5 d during the post-superoutburst phase (figure 3) may be the same phenomenon of "mini-rebrightenings" recorded in the Kepler data of V585 Lyr (Kato and Osaki 2013a).

The times of maxima of superhumps used in this study are listed in table 2.

Acknowledgements

This work was supported by JSPS KAKENHI Grant Number 21K03616. The author is grateful to the TESS team for making their data available to the public. I am grateful to Naoto Kojiguchi for helping downloading the TESS data.

List of objects in this paper

V844 Her, V585 Lyr, WZ Sge, SU UMa, SW UMa

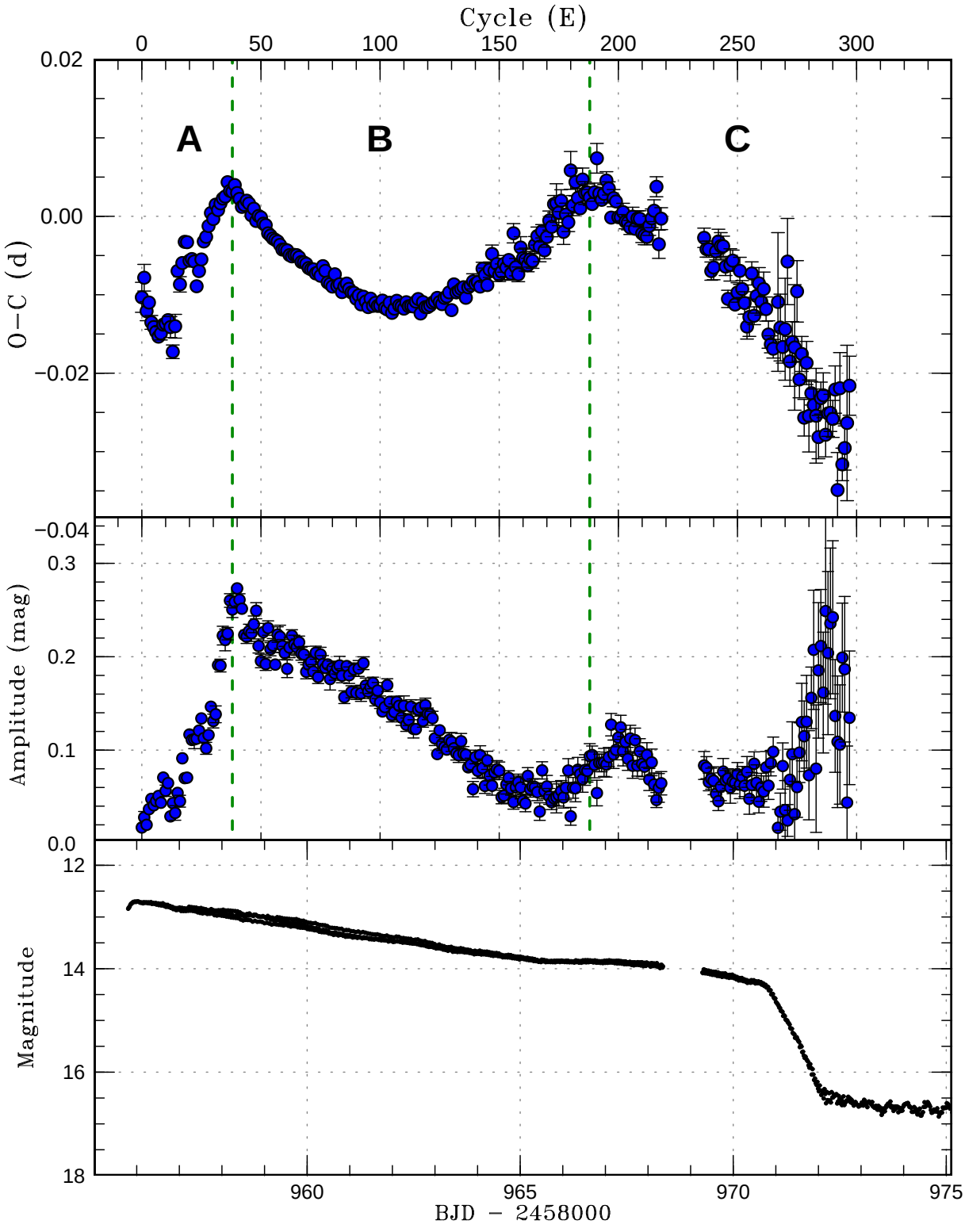

Figure 1: Superhump stages in V844 Her during the 2020 superoutburst. (Upper:) $O-C$ variation. The ephemeris of BJD(max) = 2458957.350+0.05592E was used. The data are in table 2. (Middle:) Superhump amplitude. The amplitudes grew during stage A (textbook behavior of a short-period system). They decreased during stage B, and showed a slight growth when stage C started. (Lower:) TESS light curve. The data were binned to 0.019 d. Slight brightening in stage C corresponds to the slight growth of superhumps in the middle panel.

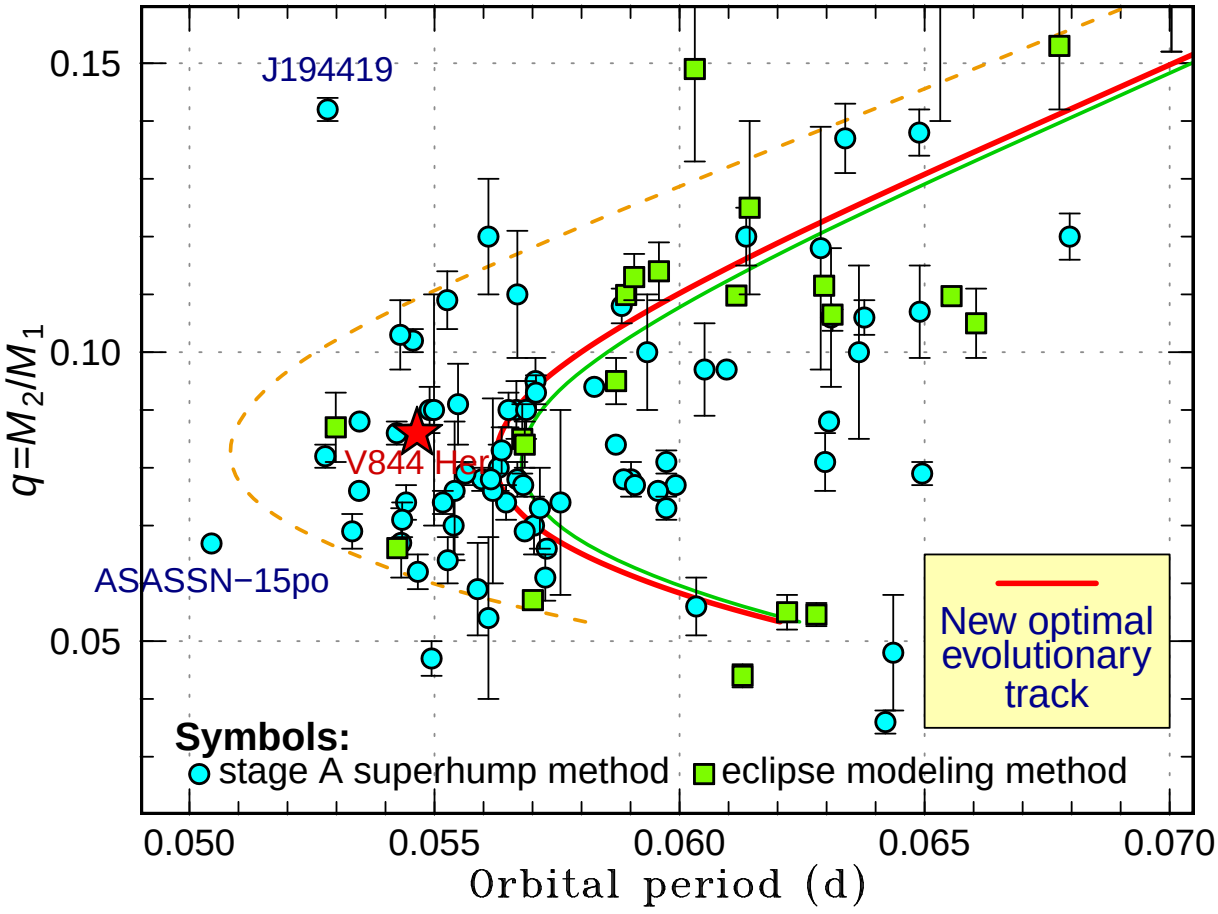

Figure 2: Location of V844 Her (filled red star) on the relation between mass ratios (q) and orbital periods ($P_{\rm orb}$) determined by the eclipse modeling method and the stage A superhump method, enlargement around the period minimum. The dashed and green solid curves represent the standard and optimal evolutionary tracks in Knigge et al. (2011), respectively. The revised optimal evolutionary track in Kato (2022) is shown by a red solid curve. See explanation in Kato (2022) for more details.

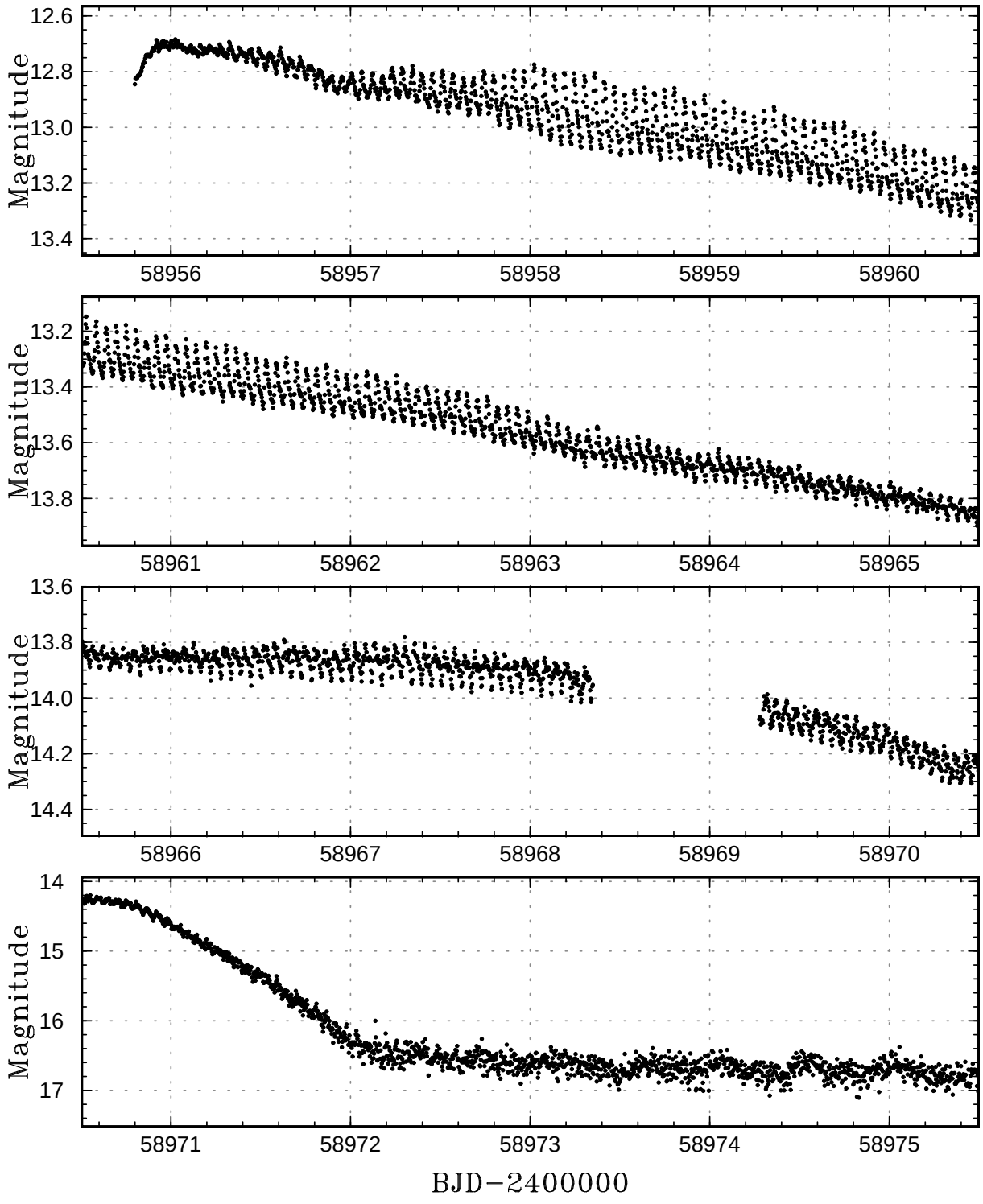

Figure 3: TESS light curve of V844 Her during the 2020 superoutburst and early post-superoutburst phase. The magnitudes were defined as $-2.5\log_{10}(\mathrm{flux}/15000)+10$. The data were binned to 0.003 d. Small wiggles with a period of $\sim$0.5 d during the post-superoutburst phase may be the same phenomenon of "mini-rebrightenings" recorded in the Kepler data of V585 Lyr (Kato and Osaki 2013a).

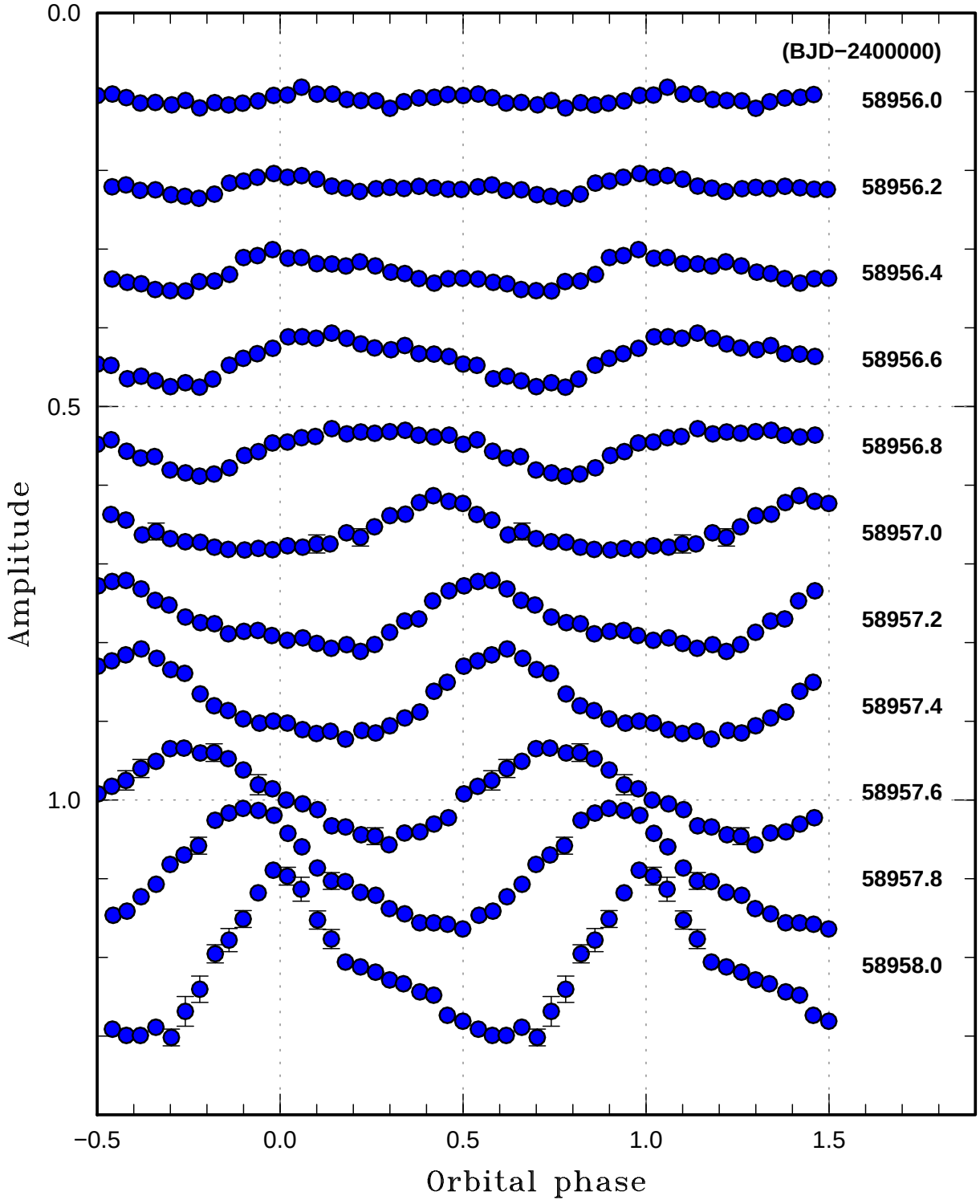

Figure 4: Variation of profiles of superhumps in the growing phase. The zero phase and orbital period were defined as BJD 2458956.000 (arbitrarily chosen) and 0.054643 d. 0.2-d segments were used whose centers are shown on the right side of the figure. After BJD 2458957.0, superhumps (stage A superhumps) with a period longer than the orbital period developed. Between BJD 2458956.0 and 2458957.0, the period was closer to the orbital one, while the average epoch was on the smooth extension of stage A superhumps (see figure 1).

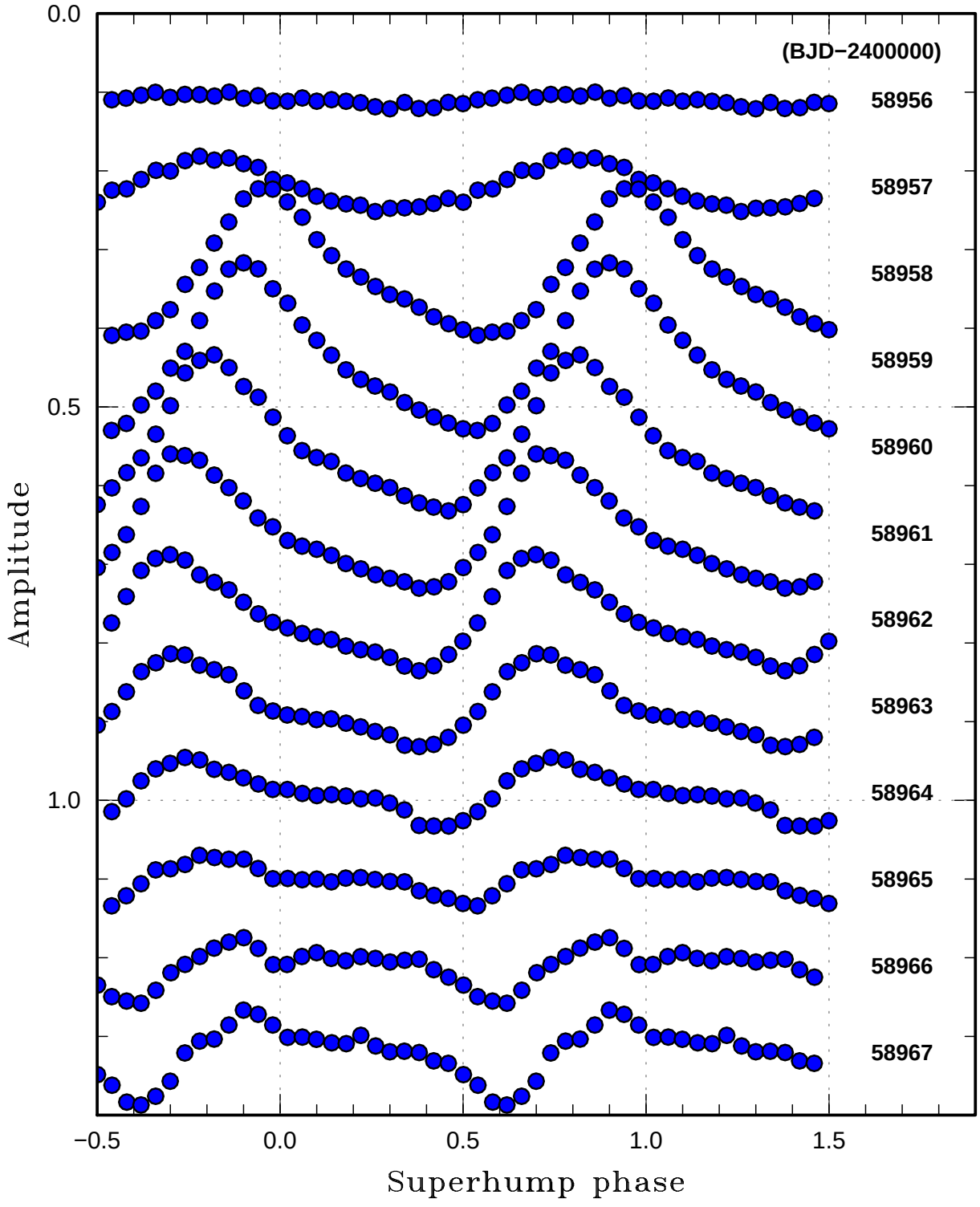

Figure 5: Variation of profiles of superhumps in stages A and B. The zero phase and superhump period were defined as BJD 2458958.2479 and 0.055592 d. 1-d segments were used whose centers are shown on the right side of the figure. Systematic variation of the peak phase corresponds to the $O-C$ variation or period change.

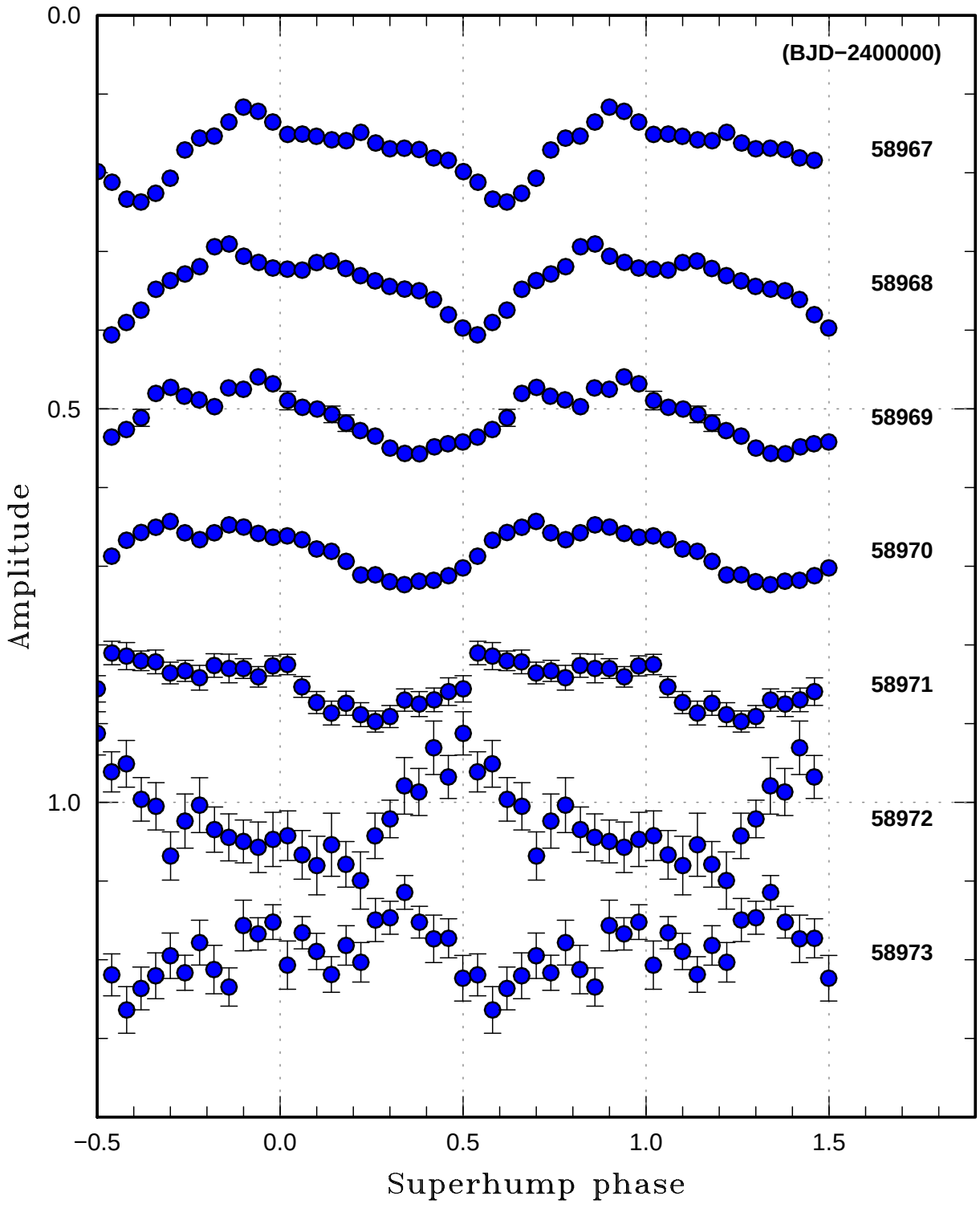

Figure 6: Variation of profiles of superhumps from stage B-C transition to the early post-superoutburst phase. The zero phase and superhump period were defined as BJD 2458958.2479 and 0.055592 d. 1-d segments were used whose centers are shown on the right side of the figure. Although post-superoutburst superhumps were visible (after BJD 2458972), they became inapparent due to flickering.

Table 2: Times of superhump maxima in V844 Her

E	T^*	error	amp†	E	T	error	amp	E	T	error	amp
0	956.1094	0.0019	0.017	47	958.7490	0.0003	0.235	94	961.3654	0.0003	0.169
1	956.1679	0.0017	0.028	48	958.8033	0.0002	0.249	95	961.4206	0.0003	0.163
2	956.2195	0.0012	0.020	49	958.8599	0.0002	0.212	96	961.4776	0.0003	0.167
3	956.2765	0.0008	0.037	50	958.9156	0.0003	0.195	97	961.5326	0.0003	0.172
4	956.3299	0.0009	0.048	51	958.9707	0.0003	0.226	98	961.5889	0.0003	0.154
5	956.3852	0.0007	0.041	52	959.0265	0.0002	0.192	99	961.6444	0.0004	0.164
6	956.4406	0.0008	0.045	53	959.0814	0.0002	0.231	100	961.7004	0.0003	0.151
7	956.4959	0.0008	0.051	54	959.1370	0.0002	0.208	101	961.7569	0.0003	0.141
8	956.5522	0.0008	0.044	55	959.1925	0.0003	0.212	102	961.8119	0.0003	0.146
9	956.6092	0.0004	0.071	56	959.2483	0.0002	0.192	103	961.8676	0.0003	0.170
10	956.6653	0.0007	0.056	57	959.3040	0.0003	0.224	104	961.9244	0.0003	0.152
11	956.7216	0.0005	0.065	58	959.3595	0.0004	0.221	105	961.9791	0.0004	0.137
12	956.7767	0.0013	0.029	59	959.4148	0.0002	0.211	106	962.0355	0.0005	0.141
13	956.8295	0.0009	0.043	60	959.4707	0.0002	0.204	107	962.0924	0.0003	0.152
14	956.8886	0.0015	0.033	61	959.5265	0.0004	0.187	108	962.1477	0.0003	0.147
15	956.9516	0.0007	0.054	62	959.5819	0.0004	0.210	109	962.2035	0.0004	0.135
16	957.0058	0.0010	0.045	63	959.6376	0.0002	0.223	110	962.2592	0.0005	0.147
17	957.0644	0.0005	0.091	64	959.6937	0.0003	0.213	111	962.3159	0.0004	0.127
18	957.1231	0.0005	0.070	65	959.7496	0.0003	0.210	112	962.3713	0.0003	0.132
19	957.1789	0.0005	0.070	66	959.8053	0.0002	0.215	113	962.4273	0.0004	0.147
20	957.2325	0.0003	0.117	67	959.8606	0.0002	0.203	114	962.4831	0.0006	0.123
21	957.2886	0.0004	0.111	68	959.9164	0.0003	0.202	115	962.5397	0.0003	0.123
22	957.3442	0.0006	0.112	69	959.9722	0.0003	0.184	116	962.5959	0.0003	0.143
23	957.3970	0.0003	0.112	70	960.0276	0.0002	0.191	117	962.6500	0.0004	0.146
24	957.4549	0.0003	0.121	71	960.0833	0.0003	0.194	118	962.7074	0.0004	0.131
25	957.5123	0.0003	0.134	72	960.1392	0.0003	0.184	119	962.7627	0.0004	0.148
26	957.5705	0.0003	0.113	73	960.1946	0.0002	0.204	120	962.8186	0.0003	0.139
27	957.6270	0.0004	0.102	74	960.2507	0.0003	0.178	121	962.8747	0.0003	0.138
28	957.6843	0.0003	0.116	75	960.3062	0.0003	0.202	122	962.9310	0.0004	0.134
29	957.7419	0.0002	0.146	76	960.3633	0.0003	0.192	123	962.9871	0.0005	0.113
30	957.7970	0.0004	0.131	77	960.4186	0.0002	0.188	124	963.0434	0.0004	0.096
31	957.8548	0.0005	0.138	78	960.4731	0.0002	0.192	125	963.0988	0.0003	0.121
32	957.9100	0.0002	0.191	79	960.5288	0.0005	0.176	126	963.1545	0.0005	0.106
33	957.9668	0.0003	0.191	80	960.5844	0.0003	0.188	127	963.2112	0.0004	0.103
34	958.0233	0.0003	0.223	81	960.6419	0.0003	0.182	128	963.2673	0.0003	0.101
35	958.0795	0.0004	0.218	82	960.6963	0.0002	0.188	129	963.3237	0.0005	0.111
36	958.1372	0.0002	0.225	83	960.7525	0.0004	0.191	130	963.3774	0.0007	0.109
37	958.1920	0.0002	0.260	84	960.8074	0.0003	0.180	131	963.4366	0.0004	0.102
38	958.2479	0.0002	0.251	85	960.8640	0.0003	0.157	132	963.4915	0.0005	0.096
39	958.3046	0.0002	0.259	86	960.9203	0.0002	0.190	133	963.5476	0.0006	0.095
40	958.3595	0.0001	0.273	87	960.9756	0.0003	0.180	134	963.6038	0.0005	0.109
41	958.4147	0.0002	0.261	88	961.0310	0.0003	0.162	135	963.6599	0.0005	0.096
42	958.4696	0.0001	0.251	89	961.0869	0.0003	0.186	136	963.7145	0.0004	0.095
43	958.5258	0.0002	0.223	90	961.1421	0.0003	0.161	137	963.7717	0.0005	0.082
44	958.5822	0.0002	0.221	91	961.1984	0.0003	0.187	138	963.8279	0.0006	0.084
45	958.6378	0.0002	0.227	92	961.2532	0.0004	0.161	139	963.8843	0.0010	0.058
46	958.6922	0.0003	0.225	93	961.3101	0.0003	0.193	140	963.9400	0.0005	0.093

*BJD$-$2458000.

†Amplitude (mag).

Table 2: Times of superhump maxima in V844 Her (continued)

E	T^*	error	amp†	E	T	error	amp	E	T	error	amp
141	963.9961	0.0008	0.078	188	966.6351	0.0010	0.093	252	970.2023	0.0011	0.072
142	964.0514	0.0007	0.095	189	966.6902	0.0007	0.095	253	970.2565	0.0014	0.062
143	964.1096	0.0008	0.081	190	966.7476	0.0012	0.084	254	970.3094	0.0016	0.077
144	964.1647	0.0009	0.062	191	966.8079	0.0019	0.054	255	970.3665	0.0025	0.048
145	964.2194	0.0008	0.089	192	966.8593	0.0008	0.086	256	970.4280	0.0015	0.063
146	964.2773	0.0010	0.073	193	966.9144	0.0008	0.086	257	970.4785	0.0011	0.085
147	964.3352	0.0011	0.062	194	966.9711	0.0012	0.087	258	970.5370	0.0022	0.065
148	964.3890	0.0007	0.076	195	967.0287	0.0011	0.085	259	970.5945	0.0020	0.045
149	964.4458	0.0008	0.080	196	967.0836	0.0008	0.093	260	970.6481	0.0017	0.060
150	964.5003	0.0008	0.078	197	967.1358	0.0007	0.127	261	970.7056	0.0022	0.056
151	964.5566	0.0010	0.050	198	967.1942	0.0011	0.096	262	970.7590	0.0015	0.081
152	964.6135	0.0011	0.051	199	967.2497	0.0008	0.100	263	970.8117	0.0017	0.062
153	964.6690	0.0011	0.063	200	967.3036	0.0006	0.113	264	970.8663	0.0011	0.086
154	964.7259	0.0008	0.070	201	967.3596	0.0008	0.124	265	970.9217	0.0012	0.098
155	964.7801	0.0009	0.059	202	967.4161	0.0011	0.099	267	971.0395	0.0088	0.017
156	964.8411	0.0012	0.044	203	967.4708	0.0009	0.109	268	971.0921	0.0043	0.034
157	964.8927	0.0011	0.060	204	967.5267	0.0009	0.091	269	971.1456	0.0020	0.083
158	964.9477	0.0009	0.066	205	967.5819	0.0009	0.112	270	971.2038	0.0065	0.036
159	965.0071	0.0014	0.060	206	967.6392	0.0012	0.083	271	971.2683	0.0055	0.025
160	965.0616	0.0011	0.046	207	967.6936	0.0008	0.111	272	971.3115	0.0032	0.068
161	965.1174	0.0015	0.043	208	967.7508	0.0009	0.083	273	971.3699	0.0026	0.096
162	965.1726	0.0009	0.072	209	967.8067	0.0010	0.099	274	971.4251	0.0080	0.031
163	965.2292	0.0010	0.058	210	967.8608	0.0012	0.085	275	971.4882	0.0039	0.060
164	965.2849	0.0009	0.061	211	967.9164	0.0012	0.082	276	971.5329	0.0023	0.097
165	965.3429	0.0011	0.060	212	967.9722	0.0010	0.095	277	971.5921	0.0022	0.130
166	965.4000	0.0011	0.055	213	968.0295	0.0012	0.069	278	971.6398	0.0023	0.115
167	965.4545	0.0019	0.034	214	968.0864	0.0012	0.087	279	971.7027	0.0027	0.130
168	965.5124	0.0009	0.078	215	968.1433	0.0014	0.063	280	971.7519	0.0046	0.073
169	965.5659	0.0011	0.056	216	968.2022	0.0013	0.047	281	971.8107	0.0015	0.156
170	965.6235	0.0013	0.061	217	968.2508	0.0018	0.060	282	971.8651	0.0020	0.207
171	965.6815	0.0012	0.050	218	968.3100	0.0014	0.065	283	971.9197	0.0060	0.080
172	965.7367	0.0013	0.044	236	969.3141	0.0012	0.084	284	971.9729	0.0028	0.185
173	965.7955	0.0011	0.048	237	969.3686	0.0010	0.081	285	972.0338	0.0020	0.211
174	965.8515	0.0025	0.050	238	969.4245	0.0010	0.066	286	972.0901	0.0029	0.162
175	965.9062	0.0016	0.052	239	969.4777	0.0012	0.069	287	972.1410	0.0028	0.249
176	965.9637	0.0014	0.056	240	969.5340	0.0016	0.067	288	972.1996	0.0029	0.204
177	966.0156	0.0016	0.049	241	969.5920	0.0011	0.053	289	972.2556	0.0024	0.236
178	966.0737	0.0015	0.060	242	969.6492	0.0016	0.045	290	972.3107	0.0024	0.242
179	966.1287	0.0012	0.078	243	969.7045	0.0017	0.061	291	972.3704	0.0030	0.137
180	966.1912	0.0024	0.029	244	969.7604	0.0013	0.077	292	972.4135	0.0048	0.109
181	966.2426	0.0013	0.060	245	969.8137	0.0011	0.068	293	972.4824	0.0045	0.106
182	966.3016	0.0018	0.059	246	969.8656	0.0011	0.070	294	972.5286	0.0021	0.199
183	966.3555	0.0012	0.079	247	969.9258	0.0021	0.060	295	972.5866	0.0028	0.187
184	966.4101	0.0008	0.074	248	969.9823	0.0013	0.066	296	972.6457	0.0099	0.044
185	966.4696	0.0015	0.069	249	970.0326	0.0008	0.065	297	972.7064	0.0038	0.135
186	966.5238	0.0015	0.079	250	970.0901	0.0012	0.074				
187	966.5798	0.0011	0.078	251	970.1487	0.0017	0.063				

*BJD−2458000.

†Amplitude (mag).

References

Antipin, S. V. (1996) Nine new variables in the η Herculis field. *IBVS* **4360**, 1

Cleveland, W. S. (1979) Robust locally weighted regression and smoothing scatterplots. *J. Amer. Statist. Assoc.* **74**, 829

Fernie, J. D. (1989) Uncertainties in period determinations. *PASP* **101**, 225

Kato, T. (2015) WZ Sge-type dwarf novae. *PASJ* **67**, 108

Kato, T. (2022) Evolution of short-period cataclysmic variables: implications from eclipse modeling and stage a superhump method (with New Year's gift). *VSOLJ Variable Star Bull.* **89**, (arXiv:2201.02945)

Kato, T. et al. (2014a) Survey of period variations of superhumps in SU UMa-type dwarf novae. VI: The fifth year (2013–2014). *PASJ* **66**, 90

Kato, T. et al. (2015) Survey of period variations of superhumps in SU UMa-type dwarf novae. VII: The sixth year (2014–2015). *PASJ* **67**, 105

Kato, T. et al. (2013) Survey of period variations of superhumps in SU UMa-type dwarf novae. IV: The fourth year (2011–2012). *PASJ* **65**, 23

Kato, T. et al. (2014b) Survey of period variations of superhumps in SU UMa-type dwarf novae. V: The fifth year (2012–2013). *PASJ* **66**, 30

Kato, T. et al. (2016) Survey of period variations of superhumps in SU UMa-type dwarf novae. VIII: The eighth year (2015-2016). *PASJ* **68**, 65

Kato, T. et al. (2009) Survey of period variations of superhumps in SU UMa-type dwarf novae. *PASJ* **61**, S395

Kato, T. et al. (2017) Survey of period variations of superhumps in SU UMa-type dwarf novae. IX. The ninth year (2016-2017). *PASJ* **69**, 75

Kato, T. et al. (2020) Survey of period variations of superhumps in SU UMa-type dwarf novae. X. The tenth year (2017). *PASJ* **72**, 14

Kato, T. et al. (2012) Survey of period variations of superhumps in SU UMa-type dwarf novae. III. The third year (2010–2011). *PASJ* **64**, 21

Kato, T. et al. (2010) Survey of Period Variations of Superhumps in SU UMa-Type Dwarf Novae. II. The Second Year (2009-2010). *PASJ* **62**, 1525

Kato, T., & Osaki, Y. (2013a) Analysis of three SU UMa-type dwarf novae in the Kepler field. *PASJ* **65**, 97

Kato, T., & Osaki, Y. (2013b) New method to estimate binary mass ratios by using superhumps. *PASJ* **65**, 115

Kato, T., & Uemura, M. (2000) CCD photometry of the 1999 superoutburst of V844 Her. *IBVS* **4902**, 1

Knigge, C., Baraffe, I., & Patterson, J. (2011) The evolution of cataclysmic variables as revealed by their donor stars. *ApJS* **194**, 28

Oizumi, S. et al. (2007) Long-term monitoring of the short period SU UMa-type dwarf nova, V844 Herculis. *PASJ* **59**, 643

Ricker, G. R. et al. (2015) Transiting Exoplanet Survey Satellite (TESS). *J. of Astron. Telescopes, Instruments, and Systems* **1**, 014003

Stellingwerf, R. F. (1978) Period determination using phase dispersion minimization. *ApJ* **224**, 953

Thorstensen, J. R., Patterson, J., Kemp, J., & Vennes, S. (2002) The dwarf novae of shortest period. *PASP* **114**, 1108

Warner, B. (1995) Cataclysmic Variable Stars (Cambridge: Cambridge University Press)

VSOLJ
c/o Keiichi Saijo National Science Museum, Ueno-Park, Tokyo Japan

Editor Seiichiro Kiyota
e-mail: skiyotax@gmail.com